J Mater Sci (2012) 47:4827–4837
DOI 10.1007/s10853-012-6341-2

The effects of environment on the dry sliding wear of eutectic $Fe_{30}Ni_{20}Mn_{35}Al_{15}$

Fanling Meng · Ian Baker · Paul R. Munroe

Received: 21 December 2011 / Accepted: 13 February 2012 / Published online: 3 March 2012

Abstract The wear of as-cast eutectic $Fe_{30}Ni_{20}Mn_{35}Al_{15}$, which consists of lamellar f.c.c. and B2 phases, was studied using pin-on-disk tribotests in four different environments: air, dry oxygen, dry argon, and a 4% hydrogen/nitrogen mixture. The counterface in all the tests was yttria-stabilized zirconia. Wear debris and wear tracks were examined in detail to investigate the surface effects during dry sliding and these were correlated with the wear properties. It was found that the wear rate was about 40% lower in tests performed under argon, compared to tests conducted in either air or oxygen. However, the wear rate was about 1000% higher when the tests were conducted in a hydrogen-containing environment. The near-surface regions of the pins were examined using transmission electron microscopy of cross-sectional specimens produced by focused ion beam milling. For tests in oxygen-containing environments, abrasive particles were produced by oxidation. These, protruded and peeled off from the matrix and mixed with the debris from the counterface, producing a combination of a two-body and three-body abrasive wear-controlled processes. In contrast, for tests under argon, plastic flow mechanisms dominated. The dramatic increase of wear in 4% hydrogen/nitrogen was due to hydrogen embrittlement, which meant that little plastic flow occurred, a feature consistent with the results of prior tensile tests.

F. Meng · I. Baker (✉)
Thayer School of Engineering, Dartmouth College,
Hanover, NH 03755, USA
e-mail: Ian.Baker@dartmouth.edu

P. R. Munroe
Electron Microscope Unit, University of New South Wales,
Sydney, NSW 2052, Australia

Introduction

Intermetallic compounds have been of considerable interest since the 1950s due to their often high strength, low density, and good oxidation and corrosion resistance. However, the brittleness at low temperature of many strongly-ordered intermetallics limits their structural application, which has led to significant efforts to improve their ductility. A novel eutectic alloy with nominal composition $Fe_{30}Ni_{20}Mn_{35}Al_{15}$, consisting of alternating B2 (ordered b.c.c.) and f.c.c. phases, has been recently found to show good room-temperature strength and significant ductility. Tensile tests at room temperature at a strain rate of $1 \times 10^{-4}\ s^{-1}$ showed a yield strength of 600 MPa, a fracture strength of 840 MPa, and an elongation of $\sim 8\%$ [1]. These excellent properties also suggest a promising future as a tribo-material that can be used in aggressive conditions. However, no work has been reported regarding the wear characteristics of $Fe_{30}Ni_{20}Mn_{35}Al_{15}$.

Because sliding contact could occur in many potential material applications, such as in seal components, it is important to study their wear behavior under sliding conditions. Dry sliding wear has been studied for a number of intermetallic compounds. Kim et al. [2] studied the room temperature dry sliding wear behavior of iron aluminides containing various aluminum contents ranging from 25 to 30 at%. They reported that the wear rate of the aluminides increased with the increase in both applied load and sliding speed, and that the wear resistance decreased with the increasing aluminum content. Microploughing and the formation and resulting detachment of surface deformation layers from the wearing surface were found to be the basic sliding wear mechanisms of these aluminide alloys. Hawk et al. [3] noted that the addition of Ti to Fe_3Al, which resulted in a two phase-microstructure, was very effective

in improving the anti-abrasive properties. They found that a $Fe_{65}Al_{25}Ti_{10}$ alloy had a wear rate approximately 40% lower than that of binary Fe_3Al alloy. This research suggests certain elemental additions can significantly change the wear properties of a material. Guan et al. [4] investigated the dry sliding wear behavior of Fe–28Al and Fe–28Al–10Ti (both in at%), and found the Ti addition could lower both the wear rate and the coefficient of friction significantly. They also reported that plastic deformation and the delamination of surface layers from the wear track, were the basic mechanisms under both mild sliding conditions, with low load (<5 N) and low speed (<0.1 m s^{-1}), and in the severe conditions with high load (>5 N) and high speed (>0.1 m s^{-1}).

The tribological properties are not only attributed to the relevant material itself, but also strongly depend on the counterface material, the environment, and other experimental conditions [2, 4]. In the present work, tests were performed in four different environments. Several studies have shown that the test environment can have a significant influence on wear of nickel aluminides and some other intermetallics. For instance, Bonda et al. [5] found that the wear rate of Ni_3Al was appreciably higher in air than in vacuum, an effect attributed to the influence of oxygen. Singh et al. [6] reported that oxidation also played a major role in the wear of a $Ti_{50}Ni_{47}Fe_3$ intermetallic alloy. The presence of surface oxides could also lower wear damage by acting as solid lubricants as well as reducing the metal to metal contact [7]. Previous work by Kennedy et al. [8, 9] showed that wear of NiAl and Ni–Al–Fe alloys increased as the amount of oxygen in the environment increases. The primary factor leading to increased wear in oxygen environments was found to be the presence of abrasive third-body wear debris composed of oxides of nickel and aluminum [8]. Also, a Ni–Al–Fe two-phase alloy showed greater wear rates than NiAl single-phase alloys, because the ductile b.c.c. precipitates, present in the alloy, facilitated shear during sliding [9]. The same phenomenon has been found for other materials containing a soft second phase [10, 11].

The effects of humidity on wear are not fully understood yet. One explanation for how humidity affects wear is that at low relative humidity water inhibits the adsorption of oxygen, reduces the rate of oxidation, and so more intermetallic alloy is at the free surface to be involved in contact during wear testing. At higher humidity, the greater amount of water adsorbed becomes sufficient to augment the protection of intermetallic alloy provided by the oxide and wear then decreases. [12]

Concerning the present alloy, Liao et al. [13] performed tensile tests of $Fe_{30}Ni_{20}Mn_{35}Al_{15}$ at different strain rates in air, oxygen, and 4% hydrogen/nitrogen. They showed that the elongation to fracture increased with increasing strain

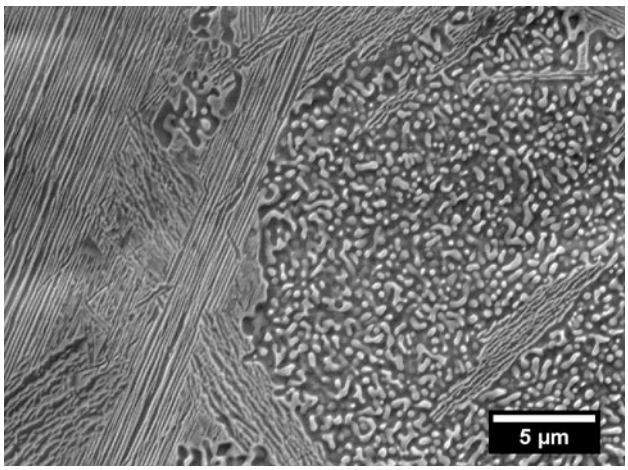

Fig. 1 Secondary electron image of as-cast $Fe_{30}Ni_{20}Mn_{35}Al_{15}$; the *dark* and *light* regions are f.c.c. and B2 phases, respectively

rates below 3×10^{-3} s^{-1} (from 0.7% at 3×10^{-6} s^{-1} to 8% at 3×10^{-4} s^{-1}) and was independent of strain rate at ~10.5% for strain rates above 3×10^{-3} s^{-1} in air. The elongation in oxygen was insensitive to strain rate and close to those tested at 3×10^{-3} s^{-1} in air, whereas the elongation in hydrogen was 4% for strain rates below 3×10^{-3} s^{-1} and increased to ~10.8% at 3×10^{-1} s^{-1}. The reduction of ductility in both air and hydrogen environment at low strain rate is attributed to hydrogen embrittlement. In air, the hydrogen can be produced by the reaction of water vapor with aluminum, which generates atomic hydrogen that subsequently assists crack nucleation by diffusing rapidly into the metal [14]. The changes in tensile properties can be reflected to changes in wear rates under different environments.

The test environment can significantly affect the wear properties and change the operative wear mechanism. This

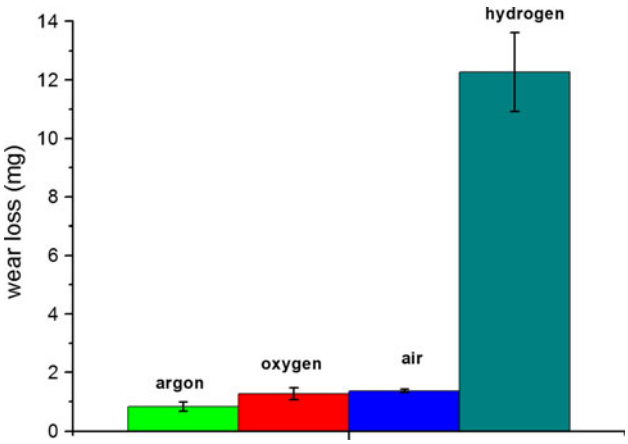

Fig. 2 Wear losses (mean value of mass loss) of eutectic $Fe_{30}Ni_{20}Mn_{35}Al_{15}$ after 1-km sliding tests in argon, air, oxygen, and 4% hydrogen/nitrogen. *Error bars* signify standard deviation from three tests

paper aims at characterizing the wear behavior of $Fe_{30}Ni_{20}Mn_{35}Al_{15}$ during dry sliding wear in a range of environments. The wear mechanisms in these different environments were also studied by scanning electron microscopy and transmission electron microscopy including X-ray microanalysis. An attempt has been made to correlate the sliding wear behavior to mechanical property changes in different environments.

Experimental

A master alloy with a nominal composition of $Fe_{30}Ni_{20}Mn_{35}Al_{15}$ was prepared by arc melting a mixture of elemental Fe, Ni, Mn, and Al with purities >99.8% under an Ar atmosphere in a water-cooled copper crucible. The resulting ~50 g button was flipped and re-melted three times to enhance homogeneity.

The alloy was polished, using increasingly fine grades of silicon carbide paper followed by 0.3 μm alumina powder to a mirror finish. The surface was etched using 4% nitric acid in water for ~5 s followed by rinsing in water. Specimens were examined using secondary electron (SE) imaging using a FEI XL-30 field emission gun (FEG) scanning electron microscope (SEM) equipped with an EDAX Li-drifted energy dispersive X-ray spectrometer (EDS) and operated at 15 kV.

For wear testing, the as-cast buttons were machined into wear pins 3-mm diameter and 6-mm length. Both ends of the pin were polished using 600-grit silicon carbide papers and finished using 0.3 μm alumina powder.

Pin-on-disk wear tests were performed against an yttria-stabilized zirconia counterface. The test system is described in detail by Johnson et al. [15]. Cylindrical pin specimens were fixed into a holder to keep them stationary and held against the rotating zirconia disk with a normal load of 23 N. All tests were conducted under a constant sliding speed of 1 m s^{-1} for a total sliding distance of 1 km. The tests were carried out at room temperature (22–25 °C) in an environmental chamber either with air or under a flow of dry argon, oxygen, or 4% hydrogen/nitrogen (vol%). Measured humidity levels in the test chamber showed a relative humidity of ~6% with flowing oxygen, argon, or 4% hydrogen/nitrogen, and a relative humidity of ~40% when tests were performed in air. Three tests were performed in each environment. Debris was collected during the wear tests using adhesive tape wrapped around the outside of the zirconia disk.

Mass measurements of the wear pins before, and after, testing provided a total loss resulting from wear. The density of the eutectic alloy, which is 7.02 g/cm^3, was determined according to Archimedes method and the weight loss was then converted to volume loss value.

The phases of the specimens both before, and after, wear testing, and the debris collected from the wear tests conducted in oxygen, air, and 4% hydrogen/nitrogen were analyzed using a Rigaku D/Max 2000 X-ray diffractometer (XRD) with Cu Kα radiation operated at 40 kV and 300 mA. Measurements were performed by step scanning 2θ from 10° to 120° with a 0.02° step size. A count time of 1 s per step was used, giving a total scan time of ~1.5 h. X-ray measurements were not performed on the pins tests in argon since there was insufficient debris.

The worn surfaces were examined using SE imaging and EDS on the FEI XL-30 FEG SEM operated at 15 kV.

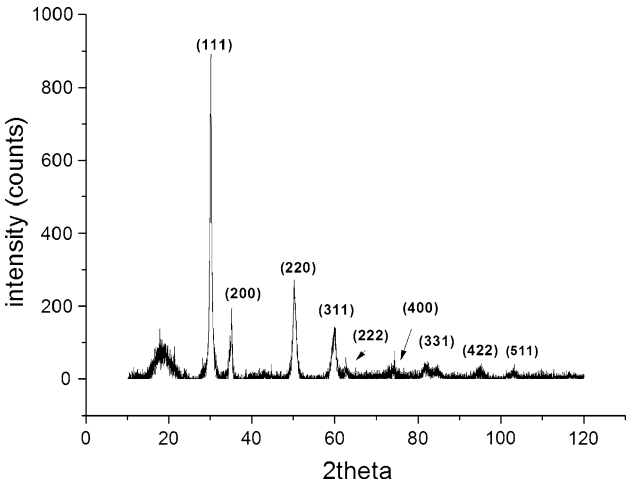

Fig. 3 XRD pattern of debris collected from the wear test performed in air, showing zirconia debris. The planes are as labeled. The broad amorphous peak around $2\theta = 30°$ is from the adhesive on the tape used to collect the debris

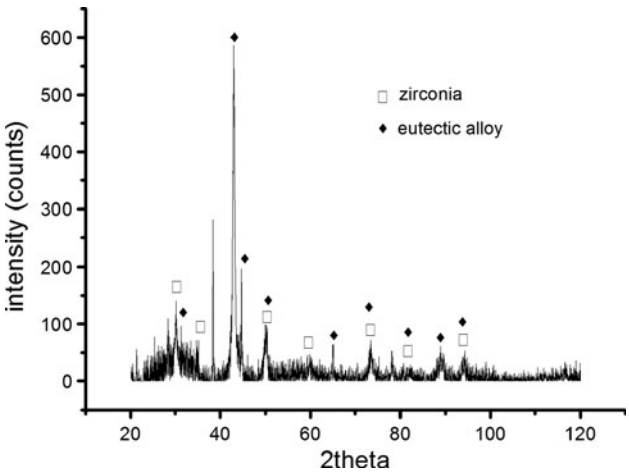

Fig. 4 XRD pattern of debris collected from the wear test performed in 4% hydrogen/nitrogen, showing peaks from both zirconia and the original eutectic alloy. The broad amorphous peak around $2\theta = 30°$ is from the adhesive on the tape used to collect the debris

Transmission electron microscope (TEM) specimens of the worn pins were prepared using a Fei Nova 200 Nanolab focused ion beam (FIB) microscope using the lift-out method [16, 17]. TEM specimens extracted from the worn pins were characterized using a Philips CM 200 TEM operating at 200 kV to which an EDS system was interfaced. Elemental X-ray maps were collected with this instrument operating in STEM mode.

The counterface after wear tests was examined using an optical microscope equipped with a digital camera.

Results and discussions

A secondary electron (SE) image of the as-cast $Fe_{30}Ni_{20}Mn_{35}Al_{15}$ showing the lamellar structure composed of alternating B2 (light) and f.c.c. (dark) phases is shown in Fig. 1. The lamellar spacing is in the order of a few hundred nanometers. This is consistent with earlier studies by Liao et al. [18], which showed that the B2 phase was 200-nm in width and separated by an f.c.c. phase 500-nm in width. EDS results showed that the B2 phase was rich in Ni and Al, while f.c.c. phase was largely composed of Fe and Mn.

The mass loss results for the pin-on-disk tests in the four different environments, i.e., air, oxygen, argon, and 4% hydrogen/nitrogen, are shown in Fig. 2. From tests in air, oxygen, and argon, it can be seen that the wear loss of the pins is considerably reduced by removing oxygen from the environment, while the humidity plays little if any role in the wear loss. Owing to hydrogen embrittlement [13], the wear loss becomes much more severe in 4% hydrogen/nitrogen, which is 10 times higher compared to the test in air. The mean mass losses of the specimens after 1-km of sliding are 0.83 mg in argon, 1.37 mg in air, 1.27 mg in oxygen, and 12.27 mg in 4% hydrogen/nitrogen. These correspond to the volumetric wear rates of 0.12 mm^3/km in argon, 0.19 mm^3/km in air, 0.18 mm^3/km in oxygen, and 1.75 mm^3/km in 4% hydrogen/nitrogen. Welsh [19] studied the wear rate of 0.5% carbon steel pin sliding 1 m s^{-1} in air against tool steel using a pin-on-ring test, and showed that the wear rate increased from 10 to 100 mm^3/km with the load increased from 10 to 20 N. Later, Kin et al. [2] reported that the wear rate of B2-structured Fe-28Al was 700 mm^3/km, using pin-on-disk

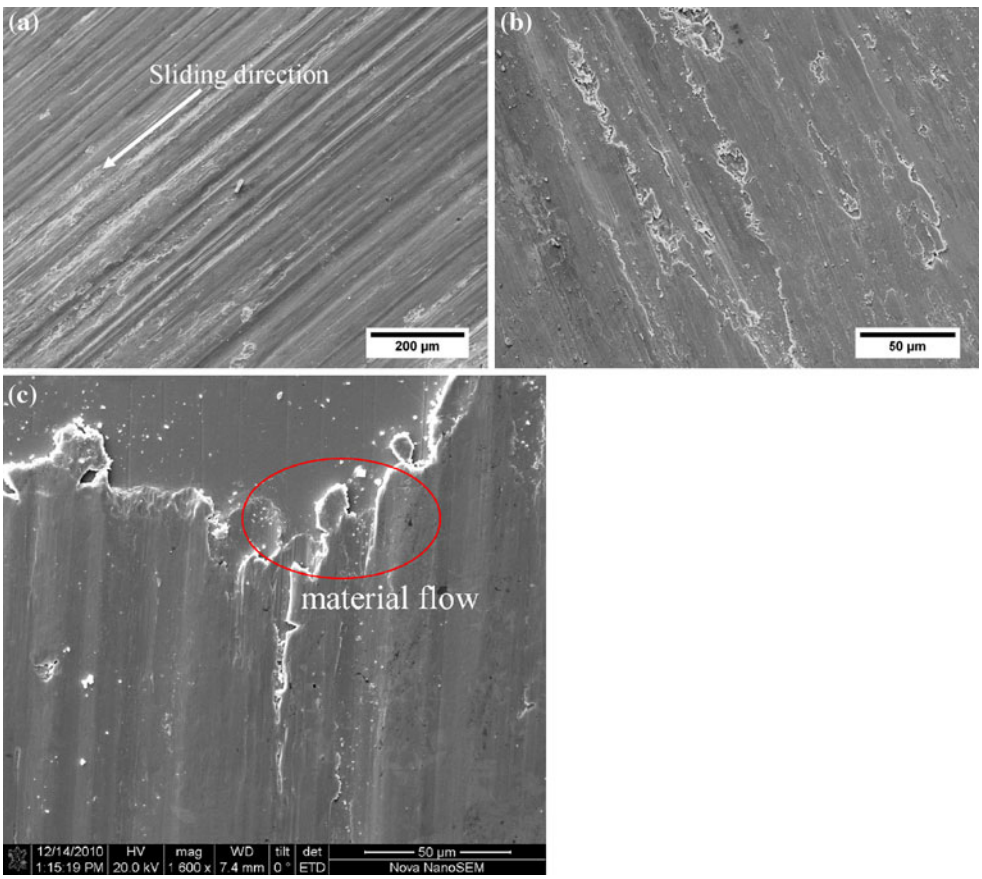

Fig. 5 Typical SE images of the surface for the pins worn in air. Note the grooves and pits after wear in (**a**–**b**), and the material flow on the trailing edge of the wear pins (**c**)

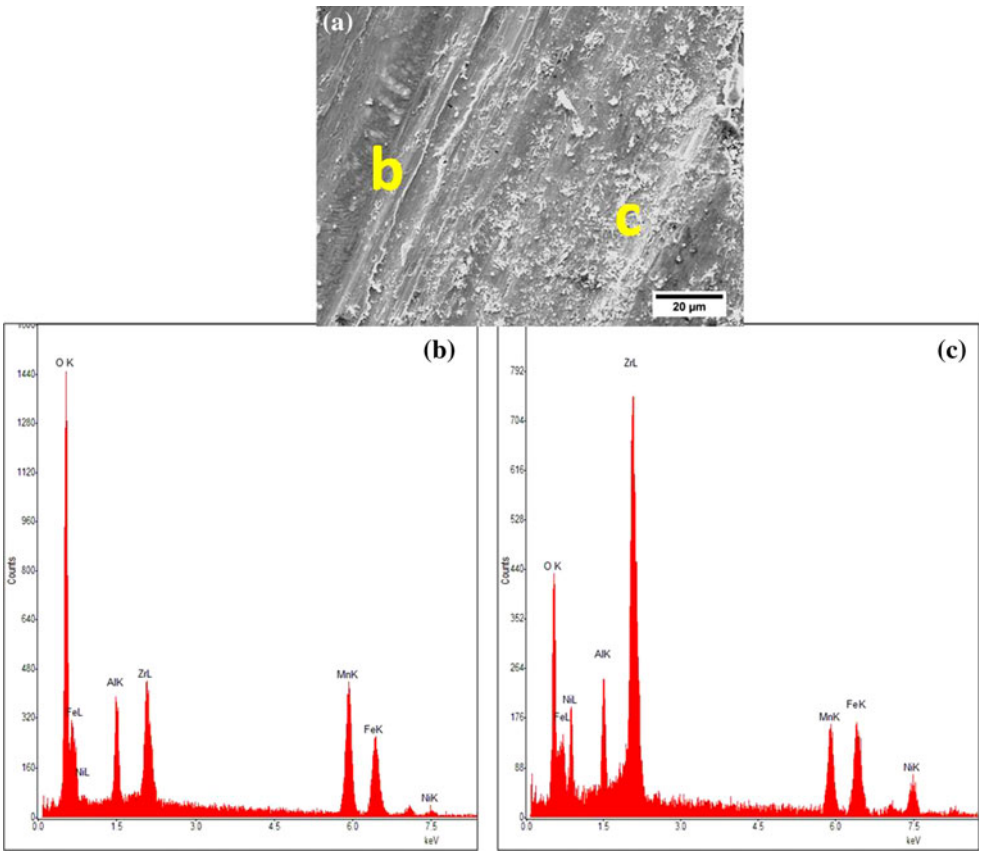

Fig. 6 SE image (**a**), showing the large quantity of oxide debris on the wear surface after a test in air, combined with EDS spectra from different regions: (**b**) is from region b and (**c**) is from region c

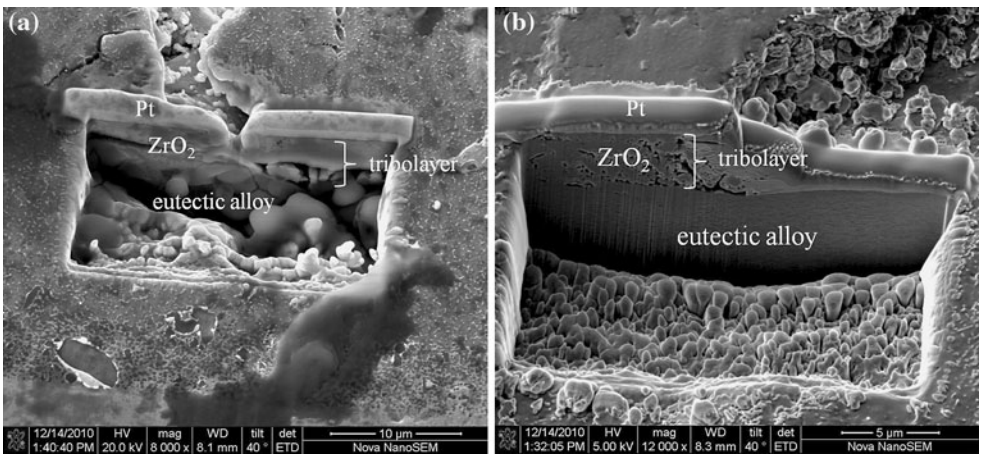

Fig. 7 SE image from pits produced using the FIB showing (**a**) a layer of eutectic alloy with a crack running above it, (**b**) zirconia layer on top with cracks. The specimen was worn in air

wear tester under load of 6.9 N and a sliding speed of 0.25 m s^{-1}. Kennedy et al. [9] investigated the wear behavior of Ni–Al–Fe alloys, and noted that wear rate of two-phase (B2 + b.c.c.) $Ni_{35}Al_{35}Fe_{30}$ and $Ni_{28}Al_{28}Fe_{44}$ was 0.25 mm^3/km and 0.46 mm^3/km in air, respectively. The comparison of wear rates between $Fe_{30}Ni_{20}Mn_{35}Al_{15}$ and these other metal materials shows enormous potential for $Fe_{30}Ni_{20}Mn_{35}Al_{15}$ applied as tribo-material in aggressive conditions. Kennedy et al. [8, 9] also showed that the wear rates in an argon environment were considerably smaller than the wear for the same materials in air or oxygen, similar to the observations here. They suggested the higher wear in air or oxygen was attributed to the creation of abrasive third-body wear debris composed of oxides of nickel and aluminum [9]. Comparing the tensile ductilities (noted in the Introduction) and the wear losses in oxygen or air with those in 4% hydrogen/nitrogen, the wear rate appears to be inversely correlated to material ductility.

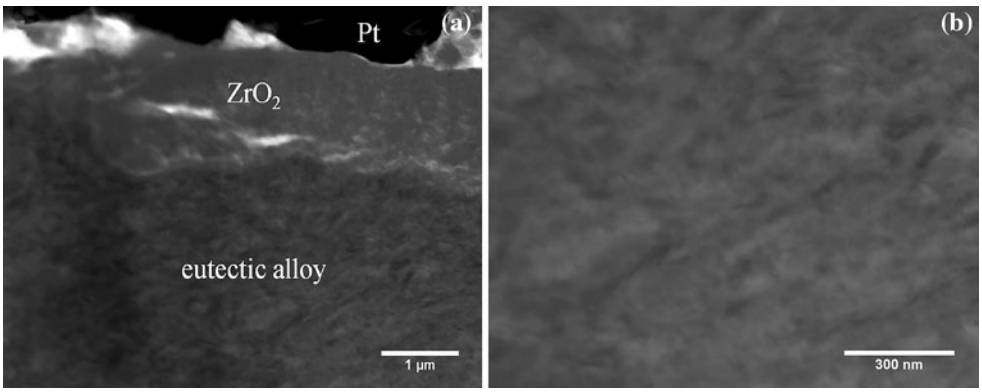

Fig. 8 Bright field TEM images of (**a**) the subsurface region in wear pin for test performed in air; (**b**) local microstructure enlarged at the outmost worn surface. The worn surface is at the top. The Pt strip was deposited in the FIB to protect the surface while milling with the FIB. The *dark area*, as labeled, is eutectic alloy. The gray regions, as marked, are zirconia

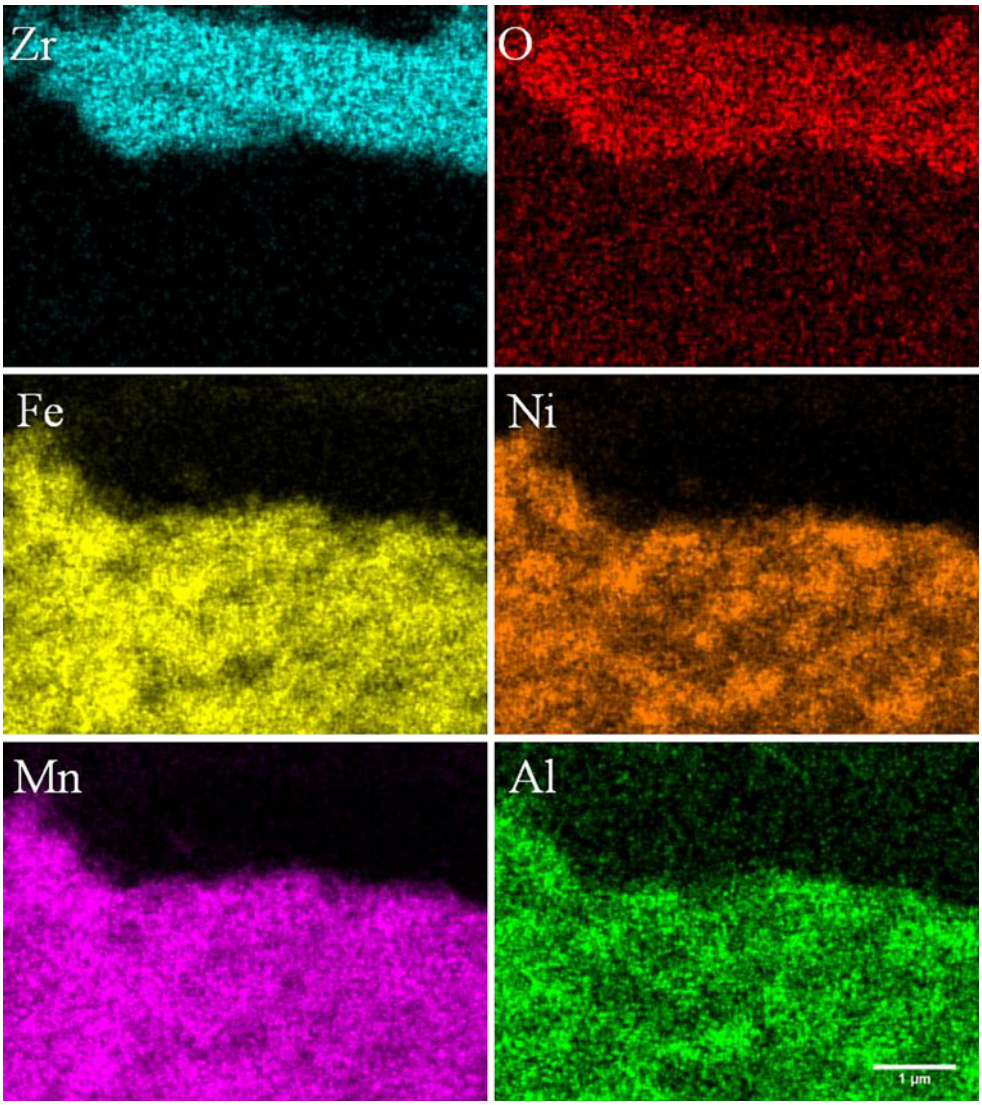

Fig. 9 X-ray elemental maps for the constituent elements from the region shown in Fig. 8a

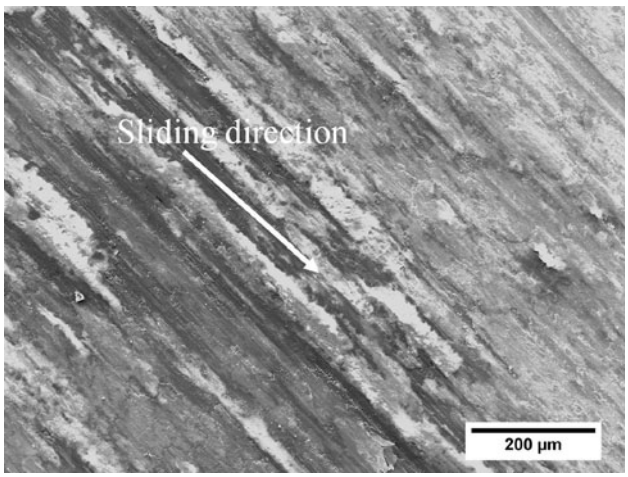

Fig. 10 Typical SE SEM image of the surface for the pins worn in oxygen. Note the grooves

XRD patterns from the debris collected from the wear test performed in air and 4% hydrogen/nitrogen are shown in Figs. 3 and 4, respectively. The debris was identified to be zirconia after testing in air (Fig. 3), which indicates large volumetric wear of the zirconia disk. XRD patterns from the debris collected from the wear test performed in oxygen are the same as that in air. However, the eutectic alloy was found in debris after testing in 4% hydrogen/nitrogen (Fig. 4). This explains the severe wear loss in hydrogen-containing environment.

SEM examination of the worn surfaces of the wear pins tested in air revealed morphologies, characteristic of abrasive wear, e.g., long parallel grooves induced by plowing (Fig. 5a), pits after material has peeled off (Fig. 5b). However, no B2 or f.c.c. phase was detected from XRD analysis of the debris, probably due to the limited volume of pullout fragments. At the trailing edge, material flow was also observed (Fig. 5c), and this further confirms the good ductility and, hence plastic flow of the eutectic alloy. In this case, both plastic deformation and abrasive wear-controlled process occurred, but the latter phenomenon predominated. In addition, deposits of debris on the pin surface were detected. EDS was used to verify the identity of these oxide particles. EDS spectra from the pins in Fig. 6 show the presence of zirconium, along with elements from the eutectic alloy on the wear surface. This is consistent with significant wear of the zirconia disk.

Using a thermoelectric technique, Moore [20] determined that frictional contact temperatures from 325 to 900 °C could occur for an iron alloy sliding over a SiC abrasive. Later, while investigating the wear of FeAl

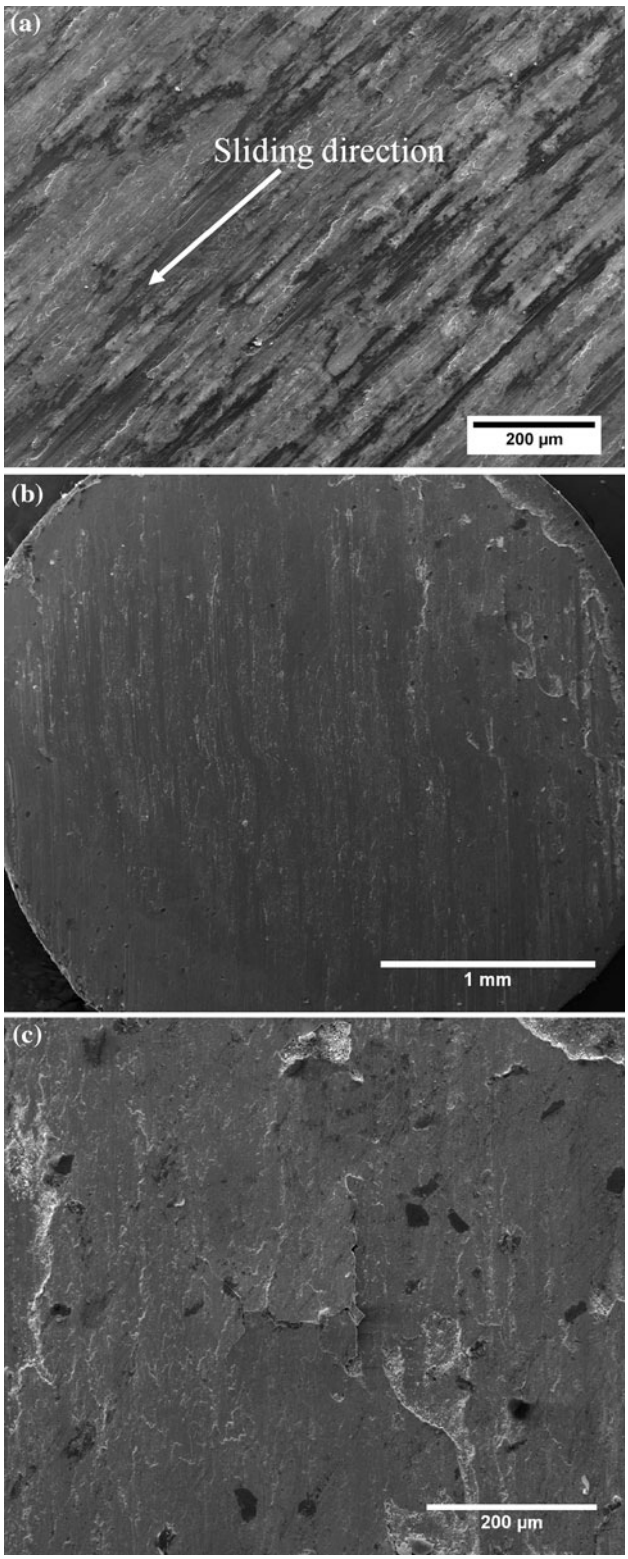

Fig. 11 SE SEM images of the surface for the pins worn in argon. Note the smearing of the surface (**a**) and pits close to the edge of sample (**b**). (**c**) is a higher magnification image of edge region

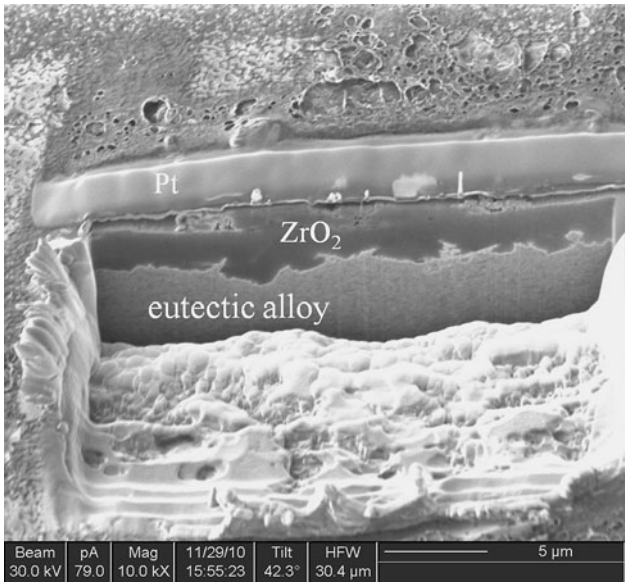

Fig. 12 SE image from FIB-prepared cross section in a specimen wear-tested under argon

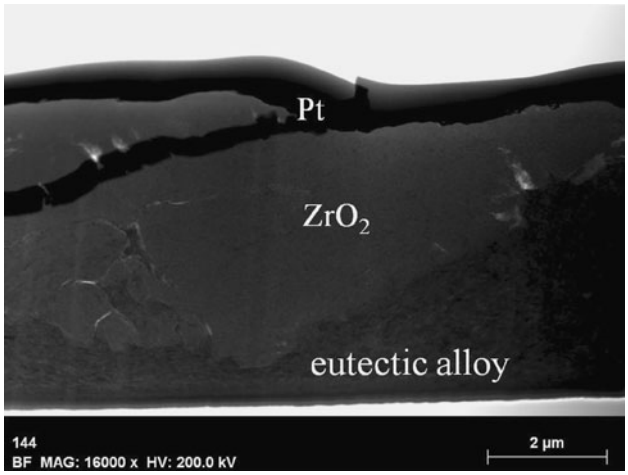

Fig. 13 Bright field TEM image of subsurface region in wear pin for tests performed in argon

intermetallics on abrasive garnet cloth of grit size 150 covered drum, Maupin et al. [21] calculated the flash temperature at the sliding interface to be approximately 380 °C. An approximate analysis of the contact temperatures present at the sliding interface during the wear tests resulting from frictional heating was also performed in this study. The methods are described by Baker et al. [17], and the calculation is in the Appendix. It was found that the contact temperatures within the contact area on the $Fe_{30}Ni_{20}Mn_{35}Al_{15}$ pin surface could reach 514 °C, a value that is sufficient to cause oxidation of pin surface. Eventually, these brittle oxides could fracture and act as third-body particles. Abrasion of zirconia by these oxides is also quite possible. Both three-body abrasion, by oxides that

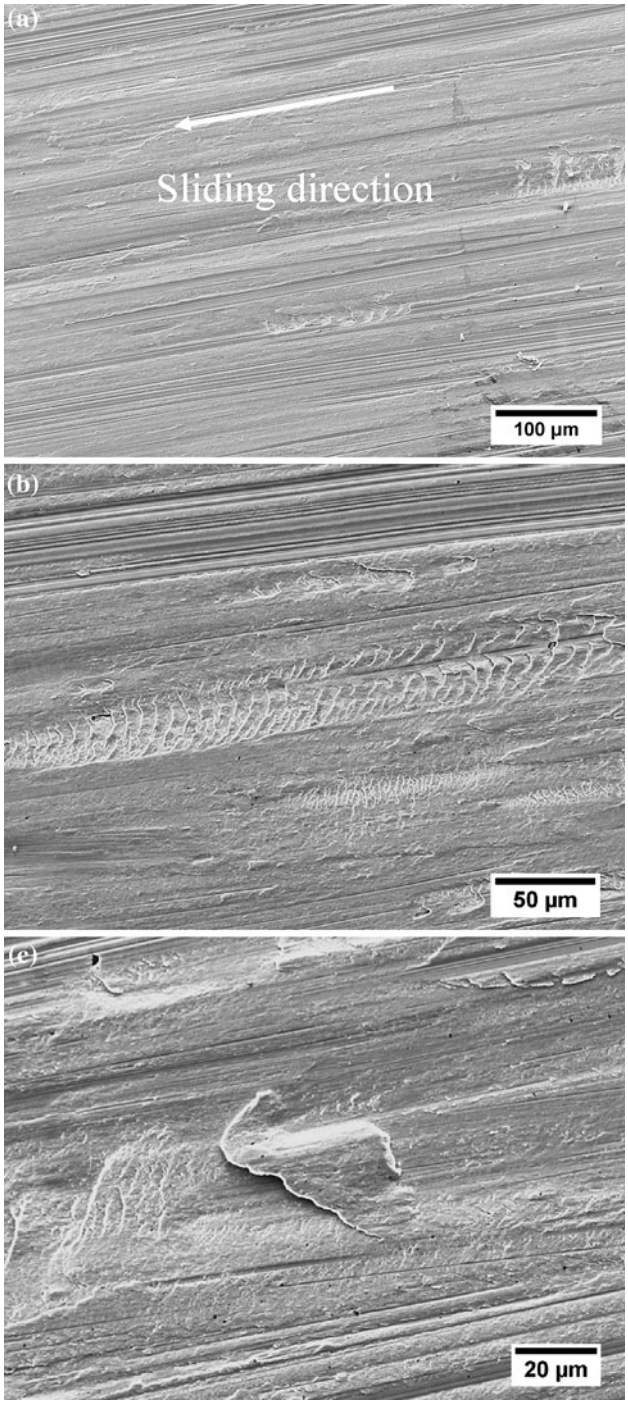

Fig. 14 SE SEM images of the surface for the pins worn in 4% hydrogen/nitrogen. Note the pits and grooves in (**a**), series of arc-shaped fractures in (**b**) and material delamination in (**c**) after wear tests

have been removed from the contacting surface tumbling between the surfaces, and two-body abrasion, by oxides embedded in the surface, are at play here. Although oxidation can be beneficial in reducing wear under mild wear conditions, it can be detrimental and lead to a considerable increase in wear [17]. If the oxide layer is thick and continuous, and adheres to the surface as a solid lubricant, it

may suppress the direct metallic contact and decrease the wear rate. On the other hand, if the oxide layer is brittle, thin, and discrete, it may act as hard third body between mating surfaces and significantly increase the wear rate [4]. Oxides formed in the eutectic $Fe_{30}Ni_{20}Mn_{35}Al_{15}$ alloy seem to correspond to the latter case.

In general, the layers underneath the worn surface of specimens, commonly associated with deformation, compaction, and fragmentation, subjected to sliding wear are called mechanically mixed layers [22], or tribolayers [23]. In the present work, FIB cross sections were prepared through the wear surfaces and the tribolayers are evident in the resulting SE images of the FIBbed pits shown in Fig. 7. This figure shows two examples of cross sections from the pin worn in air. Figure 7a shows a layer of eutectic alloy with a crack running above it, while Fig. 7b shows an area with cracks in the zirconia layer. In general, no significant subsurface cracks were evident. Baker et al. [17] showed that many subsurface cracks were found after sliding wear of eutectic Al–Si, which had an average yield stress of 130 MPa and elongation of 7% to fracture. In the present research, the eutectic $Fe_{30}Ni_{20}Mn_{35}Al_{15}$ alloy has higher strength and ductility, which could be the reason for the lack of subsurface cracks.

A bright field TEM image of the material close to the worn surface of the pin tested in air is shown in Fig. 8, while Fig. 9 shows corresponding elemental X-ray maps. An interesting feature is the presence of the zirconia layer on the worn surface of the pin. This can explain the two-body abrasion acting in the wear process.

Pins that were tested in oxygen presented a behavior largely similar to those of the pins tested in air, but the grooves were indistinct and less debris were present on the surface, see Fig. 10. FIBbed cross sections from the pins tested in oxygen showed that subsurface cracks were not present.

Compared to the results from the oxygen-containing environment, the worn surface of the specimen tested in argon was relatively smooth and free from oxides (Fig. 11a). Smearing of the wear tracks occurred, but there were still some pits where materials have been pulled out of the surface on the very edge of the sample (Fig. 11b), and an enlarged image of the edge region is also shown as Fig. 11c.

A FIB cross section from the wear track of the pin tested under argon is shown in Fig. 12. We can see a zirconia layer on top of the eutectic alloy. The corresponding bright field TEM image of the near-surface region of a specimen wear-tested under argon shows the same texture in Fig. 13. X-ray elemental maps of the same area show that the composition of the surface is similar to specimens tested in air. It seems that plastic deformation predominates when the tests were performed in argon.

The worn surface of the specimen tested in 4% hydrogen/nitrogen is shown in Fig. 14, where deep grooves and pits, indicating abrasion wear are evident. The debris is mainly pieces of the eutectic alloy. X-ray elemental maps

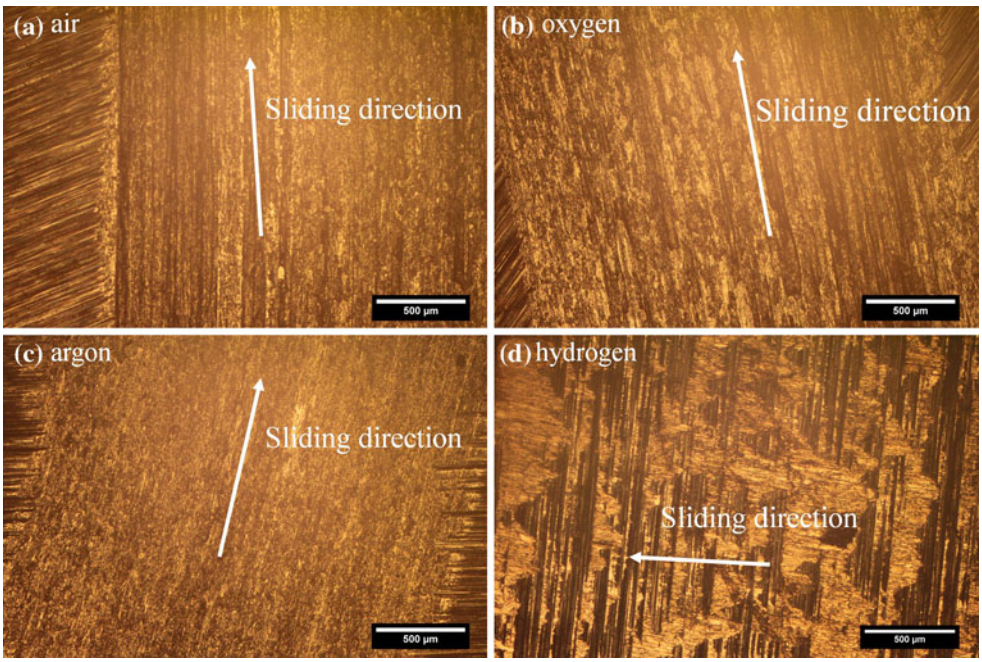

Fig. 15 Optical micrographs showing morphologies of the disk after sliding performed in different environments: (**a**) air, (**b**) oxygen, (**c**) argon, and (**d**) 4% hydrogen/nitrogen

were not acquired from the pin tested in hydrogen, since it appeared that material was largely the eutectic alloy fractured from the end of the wear pin.

A wear mechanism for metals in a hydrogen environment was suggested by Jones et al. [24], when studying the wear properties of titanium in different gas environments. They reported that the increased wear rate in dry hydrogen was due to accelerated surface fatigue. In aluminum-containing alloys, reactive hydrogen atoms can be formed from moisture in the air and the resulting atomic hydrogen can diffuse into metal rapidly, which will assist crack nucleation [25]. The decrease in ductility due to hydrogen can be significant, e.g., Fe-39.8 at% Al single crystal has an elongation to fracture of ~10% in dry oxygen, but shows only ~0.7% elongation when tested in air [26]. For wear tests of $Fe_{30}Ni_{20}Mn_{35}Al_{15}$ in 4% hydrogen/nitrogen, arc-shaped fractures (Fig. 14b) and the pieces of material delamination (Fig. 14c) were found on the wear surface, while the same phenomenon was not observed for wear tests in other environments. The parts were most likely broken away after cracks propagating into the asperity reached sufficient depth to cause detachment [24]. In this case, the wear rate was increased by more rapid crack nucleation in the asperities leading to fatigue deterioration of the asperities during the wear process. So, the dramatic increase of wear rate of $Fe_{30}Ni_{20}Mn_{35}Al_{15}$ in 4% hydrogen/nitrogen was due to hydrogen embrittlement.

Figure 15 shows the surface morphologies of the zirconia disk counterface after wear tests in different environments. For tests in air, oxygen, and argon, the wear track completely interrupts the pattern of the polished markings on the disk. This arose from a combination of the wear pin smoothing out the disk by breaking down asperities, and some debris becoming welded onto the zirconia surface. However, for the tests in 4% hydrogen/nitrogen, the polish markings were still visible.

Based on all the above results, the wear process of the eutectic $Fe_{30}Ni_{20}Mn_{35}Al_{15}$ material against zirconia appears to be very much dependent on the environment in which the tests are carried out. In dry argon, wear of $Fe_{30}Ni_{20}Mn_{35}Al_{15}$ takes place by near-surface deformation and damage accumulation. In an oxygen-containing environment, however, the wear process is abetted by oxidation of the eutectic material resulting from frictional heating, followed by pull-out of oxide particles, which then act as abrasive third bodies to abrade the zirconia counterface. The resulting zirconium oxide particles can become pulverized and mixed into the mechanically mixed layer on the surface of the eutectic material. In a hydrogen-containing environment, hydrogen embrittlement will lead to dramatic increase of wear rate. Damage to the mechanically mixed layer can result in the production of wear particles from the eutectic material.

Conclusions

The effects of environment on the tribological behavior of the eutectic alloy $Fe_{30}Ni_{20}Mn_{35}Al_{15}$, which consists of lamellar f.c.c. and B2 phases, were investigated using pin-on-disk wear tests in four different environments, i.e., air, dry oxygen, dry argon, and a 4% hydrogen/nitrogen mixture. Based on the experimental results, the following conclusions can be drawn:

1. Compared to testing in argon, the wear rate of the specimens increased when oxygen was present.
2. The effect of water vapor on the wear rate in oxygen - containing environments was small or non-existent.
3. A number of pits due to material pullout were present on the worn surface of the pin tested in the oxygen-containing environments, while a relatively smooth worn surface was observed in the specimens tested in argon.
4. For the tests in oxygen-containing environments, abrasive particles, induced by oxidation, protruded and peeled off from the matrix and together with the debris from the counterface, led to a combination of two-body and three-body abrasion, indicating an abrasive wear-controlled process. In contrast, under argon, plastic flow mechanisms dominated the wear behavior.
5. Hydrogen embrittlement can lead to dramatic increase of wear loss by causing more rapid crack nucleation of the asperities.

Acknowledgements This research was supported by National Science Foundation (NSF) Award DMR-0905229. Any opinions, findings, and conclusions or recommendations expressed in this material are those of the authors' and do not necessarily reflect the views of NSF. We would like to acknowledge technical help from Dr. Charles Daghlian.

Appendix: Calculation of contact area and contact temperature

Operating conditions:

Normal load $w = 23$ N	Sliding velocity $V = 1$ m s^{-1}
Average friction coefficient (measured) $\mu = 0.15$	Pin radius $r = 1.5$ mm

Material properties (*measured, data of zirconia is from [27])

	Zirconia (material 1)	As-cast $Fe_{30}Ni_{20}Mn_{35}Al_{15}$ (material 2)
H Hardness (GPa)	12.7	3*
E Modulus of elasticity (GPa)	290	120*
ρ Density (kg/m^3)	6100	7020*
υ Poisson's ratio	0.24	0.33
K Thermal conductivity (W/m K)	1.8	9.3*
C Specific heat (J/kg K)	630	

Contact geometry (assuming Hertzian contact [28])

Radius of contact circle $a = \left(\frac{3wr}{4E}\right)^{1/3}$

where $\frac{1}{E} = \frac{1-\upsilon_1^2}{E_1} + \frac{1-\upsilon_2^2}{E_2}$ (E_1, E_2 are the moduli of elasticity for material 1 and material 2, respectively, while υ_1 and υ_2 are the Poisson's ratio for material 1 and material 2, respectively)

Assume stationary pin (material 2) and moving flat Zirconia disk (material 1)

$$\Delta T_{\max} = \frac{1.31a\mu pV}{\sqrt{\pi}(K_1\sqrt{1.2344 + P_{e1}} + K_2\sqrt{1.2344 + P_{e2}})} = 489^{\circ}C$$

where the Peclet number $P_{e1} = \frac{Va\rho_1 C_1}{2K_1} = 70$ (V is the sliding velocity of disk, while ρ_1, C_1, and K_1 is the density, specific heat and thermal conductivity of material 1, respectively), and $P_{e2} = \frac{V_2 a\rho_2 C_2}{2K_2} = 0$ (V_2 is the sliding velocity of pin, while ρ_2, C_2, and K_2 is the density, specific heat and thermal conductivity of material 2, respectively), $p = \frac{w}{\pi a^2}$

Given that the tests were conducted at room temperature (about 25 °C), the surface temperature at the center of the Hertzian contact area was 514 °C.

References

1. Liao Y (2009) Doctoral dissertation, Dartmouth College
2. Kim YS, Kim YH (1998) Mater Sci Eng A 258:319
3. Hawk JA, Alman DE (1997) Mater Sci Eng A 239–240:899
4. Guan XS, Iwasaki K, Kishi K, Yamamoto M, Tanaka R (2004) Mater Sci Eng A 366:127
5. Rao Bonda N, Rigney DA (1989) Proc MRS 133:585
6. Singh J, Alpas AT (1995) Wear 191–183:302
7. Kato H, Eyre TS, Ralph B (1994) Acta Metal Mater 42:1703
8. Kennedy FE, George M, Baker I, Johnson BJ, Chang N (1995) Proceedings of the international tribology conference, Yokohama, I, p. 337
9. Munroe PR, George M, Baker I, Kennedy FE (2002) Mater Sci Eng A 325:1
10. Kennedy FE, Voss DA (1979) A re-examination of the wear of leaded brass on hardened steel. Wear of Materials ASME, New York
11. Kennedy FE, Hauck KK, Grotelueschen LP (1986) In: Dowson D (ed) Mechanisms and surface distress. Butterworths, London, p 67
12. Lancaster JK (1990) Tribol Int 23:372
13. Liao Y, Meng F, Baker I (2011) Intermetallics 19:1533
14. Liu CT, Lee EH, Mckamey CG (1989) Scr Metall 23:875
15. Johnson BJ, Kennedy FE, Baker I (1996) Wear 192:241
16. Giannuzzi LA, Stevie FA (1999) Micron 30:197
17. Baker I, Sun Y, Kennedy FE, Munroe PR (2010) J Mater Sci 45:969. doi:10.1007/s10853-009-4027-1
18. Liao Y, Baker I (2008) Mater Charact 59:1546
19. Welsh NC (1965) Phil Trans R Soc Lond A 257:51
20. Moore MA (1971) Wear 17:51
21. Maupin HE, Wilson RD, Hawk JA (1993) Wear 162–164:432
22. Rigney DA (2000) Wear 245:1
23. Li J, Elmadagli M, Gertsman VY, Lo J, Alpas AT (2006) Mater Sci Eng A 421:317
24. Jones JW, Wert JJ (1975) Wear 32:363
25. Stolofl NS, Liu CT (1994) Intermetallics 2:75
26. Nathal MV (1995) Intermetallics 3:77
27. Bhushan B, Gupta BK (1991) Handbook of tribology. McGraw-Hill, New York, p 4.71
28. Hutchings IM (1992) Tribology, friction and wear of engineering materials. CRC Press, Boca Raton, p 14